Science of the Total Environment 820 (2022) 153185

Contents lists available at ScienceDirect

Science of the Total Environment

journal homepage: www.elsevier.com/locate/scitotenv

Canopy structure and phenology modulate the impacts of solar radiation on C and N dynamics during litter decomposition in a temperate forest

Qing-Wei Wang [a,b,*], Thomas Matthew Robson [c], Marta Pieristè [c,d], Tanaka Kenta [e], Wangming Zhou [a], Hiroko Kurokawa [b]

[a] CAS Key Laboratory of Forest Ecology and Management, Institute of Applied Ecology, Chinese Academy of Sciences, Shenyang 110016, China
[b] Forestry and Forest Products Research Institute, 1 Matsunosato, Tsukuba, Ibaraki 305-8687, Japan
[c] Organismal and Evolutionary Biology, Viikki Plant Science Centre (ViPS), University of Helsinki, Helsinki 00014, Finland
[d] Normandie Univ, UNIROUEN, INRAE, ECODIV, Rouen 76000, France
[e] Sugadaira Research Station, Mountain Science Center, University of Tsukuba, Nagano, Japan

HIGHLIGHTS

- Sunlight drives nutrient dynamics below a forest canopy.
- Blue light increases the loss of litter C and lignin in the forest gap.
- UV-B radiation promotes litter C loss in the forest understorey.
- Litter N tends to be mineralized in the gap but immobilized in the understorey.

GRAPHICAL ABSTRACT

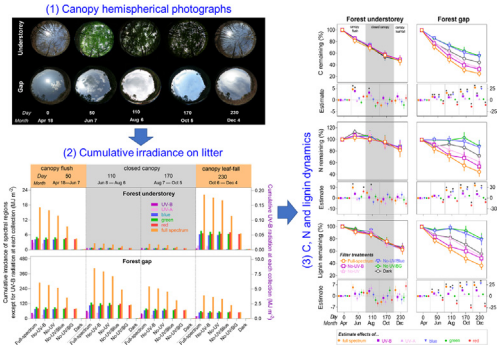

ARTICLE INFO

Article history:
Received 12 August 2021
Received in revised form 12 January 2022
Accepted 12 January 2022
Available online 19 January 2022

Editor: Manuel Esteban Lucas-Borja

Keywords:
Mesic ecosystems
Canopy cover
Carbon loss
Nutrient dynamics
Photodegradation

ABSTRACT

Decomposition of plant organic matter plays a key role in the terrestrial biogeochemical cycles. Sunlight has recently been identified as an important contributor to carbon [C] turnover through photodegradation, accelerating decomposition even in forest ecosystems where understorey solar irradiance remains relatively low. However, it is uncertain how C and nutrients dynamics respond to fluctuations in solar spectral irradiance caused by canopy structure (understorey vs. gaps) and season (open vs. closed canopy phenology). Spectral-attenuation treatments were used to compare litter decomposition over eight months, covering canopy phenology, in a temperate deciduous forest and an adjacent gap. Exposure to the full spectrum of sunlight increased the loss of litter C and lignin by 75% and 64% in the forest gap, and blue light was responsible for respectively 27% and 42% of that loss. Whereas in the understorey, C and lignin loss were similar among spectral-attenuation treatments over the experimental period, except prior to and during spring canopy flush when exposure to the full spectrum of sunlight promoted C loss by 15% overall, 80% of which was attributable to ultraviolet-B (UV-B) radiation. Nitrogen [N] was immobilized in the understorey during canopy flush before the canopy completely closed but N was swiftly released during canopy leaf-fall. Our study suggests that blue-driven photodegradation plays an important role in lignin decomposition and N dynamics in canopy gaps, whereas seasonal canopy phenology affecting sunlight reaching the forest floor drastically changes patterns of C and N in litter during decomposition. Hence, including sunlight dynamics driven by canopy structure and phenology would improve estimates of biogeochemical cycling in forests responding to changes in climate and land-use.

* Corresponding author at: CAS Key Laboratory of Forest Ecology and Management, Institute of Applied Ecology, Chinese Academy of Sciences, Shenyang 110016, China.
E-mail address: wangqingwei@iae.ac.cn (Q.-W. Wang).

http://dx.doi.org/10.1016/j.scitotenv.2022.153185

1. Introduction

Litter decomposition is essential for soil fertility, the sequestration of organic carbon in the soil, and the release of essential nutrients for plants and microbes, consequently it determines global C cycling and maintains ecosystem functioning (Schlesinger and Bernhardt, 2013). Solar radiation has been recognized as an abiotic factor that accelerates litter decomposition via photodegradation in arid and semi-arid ecosystems (Austin and Vivanco, 2006; Brandt et al., 2009; King et al., 2012; Song et al., 2013; Adair et al., 2017; Berenstecher et al., 2020). Its inclusion may challenge established models of the controls on C turnover and nutrient cycling driven by litter quality and climate (Parton et al., 2007). However, knowledge of the relative importance of photodegradation among processes driving C and N dynamics in semi-arid and arid ecosystems is not necessarily applicable to mesic ecosystems, particularly temperate deciduous forests where the light environment is dynamic and heterogenous due to canopy phenology (i.e., the annual progression through canopy flush, closed canopy, leaf-fall, and open canopy).

In the deciduous forests, the amount of understorey solar irradiance and its spectral quality vary greatly with changing canopy phenology. For instance, understorey solar irradiance of photosynthetically active radiation (PAR) at the forest floor can amount to ca. 60% and 35% of that above the canopy before leaf flush and after leaf-fall, respectively (Baldocchi et al., 1984; Augspurger et al., 2005). In comparison, under a closed canopy in summer, the understorey PAR is less than 1% of above-canopy PAR (Hertel et al., 2011). Moreover, solar spectral composition between 280 nm and 700 nm varies dramatically over the whole season, due to wavelength-selective absorption, reflection, and transmission of photons by canopy leaves (Hertel et al., 2012; Hartikainen et al., 2018). Blue (400–500 nm) and red light (600–700 nm) are preferentially absorbed, while green light (500–600 nm) penetrates deeper into the forest understorey (Durand et al., 2021; Hertel et al., 2012;). Relative to PAR, shorter wavelengths, i.e., ultraviolet-B (UV-B, 280–315 nm) and UV-A (315–400 nm) radiation are enriched in diffuse radiation and hence understorey shade due to their greater scattering by the atmosphere (Flint and Caldwell, 1998; Hartikainen et al., 2018). Furthermore, natural or human disturbances including wind, tree mortality and harvesting, create heterogeneity in forest structure (e.g. gaps) (Nakashizuka and Matsumoto, 2002; Čada et al., 2016), which further modify the characteristics of understorey solar irradiance.

Solar irradiance modulates litter decomposition processes through photodegradation, which mainly consists of direct photomineralization and indirect photofacilitation (Gallo et al., 2009; King et al., 2012; Almagro et al., 2015; Liu et al., 2018). Photomineralization represents the breakdown of complex macromolecules from dead organic matter operated by UV radiation and blue-green light (Austin and Vivanco, 2006; Brandt et al., 2009; Austin and Ballaré, 2010). Lignin is a major constituent of plant litter and its photomineralization driven by blue light may be a major contributor to photodegradation (Austin and Ballaré, 2010; Wang et al., 2021). High lignin content can limit early-phase microbial decomposition of litter; although lignin can be broken down by the extracellular enzymes synthesized by fungi during the latter stages of decomposition (Swift et al., 1979). Some studies indicate that cellulose is more susceptible to photomineralisation than lignin, e.g. as found in *Bromus diandrus* which has high cellulose content (40%) and low lignin content (3%) (Lin and King, 2014). These inconsistencies in the relative lignin and cellulose content of litter of diverse origins underpin some of the variation found in photomineralization.

A body of evidence has found that solar radiation promotes litter C turnover in drylands, mainly through photomineralization, leading to considerable CO_2 emission (nearly 40% of litter C is lost as CO_2) (Day and Bliss, 2020; Méndez et al., 2019). In contrast to lignin, a high litter N content promotes early-stage decomposition by stimulating the growth and activities of microbes that degrade labile compounds (Keyser et al., 1978), and result in N immobilization when the moisture is favorable (Predick et al., 2018). However, N release tends to be higher in litter exposed to solar radiation than in shaded litter (Asao et al., 2018; Ball et al., 2019): this was the case for litter suspended above the soil (equivalent to standing dead material) which receives more incident irradiance on its surface compared with litter lying on the soil which has greater potential for colonisation and biotic interactions.

Changes to litter chemistry caused by photomineralisation increase the availability of carbohydrates to hydrolytic enzymes and accelerate biotic degradation, known as photofacilitation (or photopriming) (Foereid et al., 2010; Baker and Allison, 2015; Day et al., 2015; Wang et al., 2015; Austin et al., 2016). On the other hand, UV-B radiation can limit litter decomposition by inhibiting microbial activity (photoinhibition) (Verhoef et al., 2000; Pancotto et al., 2003; Uselman et al., 2011; Pieristè et al., 2020a), which counteracts the acceleration of decomposition caused by photopriming. This antagonism may explain why UV-B photodegradation is not detected in some experimental (Song et al., 2013; Marinho et al., 2020) and modelling studies (Foereid et al., 2011). Hence, a better understanding of the role of solar radiation in C turnover and nutrient dynamics within forest canopies is required to refine estimates of global C cycling and its response to climate change.

There is increasing evidence that photodegradation contributes to litter decomposition in mesic ecosystems, e.g. tropical (Marinho et al., 2020), subtropical (Ma et al., 2017), temperate (Wang et al., 2021), and boreal forests (Pieristè et al., 2019; Pieristè et al., 2020a; Pieristè et al., 2020b), though solar irradiance remains relatively low in the shaded understorey of all forest ecosystems. Spatial and temporal fluctuations in the microenvironment (radiation, temperature and moisture) of heterogenous forests due to canopy dynamics (e.g., canopy phenology, gap creation) may significantly modulate litter decay rates and fluxes of nutrients through photodegradation. For instance, Pieristè et al. (2019, 2020a) found that understorey UV-A radiation and blue light can accelerate decomposition and C loss compared to other spectral regions, perhaps through lignin photodegradation which promotes photopriming under shady, cool, and moist conditions. A recent field experiment conducted in a forest gap found exposure to full solar spectral irradiance to increase decomposition rates by nearly 120% compared to darkness (Wang et al., 2021). Such an unexpectedly high relative contribution of photodegradation to decomposition in forest gaps was even greater than that reported for semi-arid ecosystems (Austin and Vivanco, 2006; Berenstecher et al., 2020). This suggests that when unattenuated by the canopy, the environment in these moist temperate biomes is favorable for ambient solar radiation to accelerate litter decomposition, most likely through lignin photomineralization (Keiser et al., 2021; Mao et al., 2018). To the best of our knowledge, however, only two studies have examined lignin photodegradation in forest ecosystems. These were conducted in common gardens and reported that lignin dynamics did not appear to respond to UV-B (Marinho et al., 2020) or UV radiation (Song et al., 2014). Little is known about how understorey solar radiation, modified by seasonality, drives litter C turnover and associated nutrient dynamics on the forest floor in an ecological context.

This study extends that of Wang et al., 2021, where the response of litter decomposition rate to photodegradation, forest canopy structure and season was assessed. These results highlighted the role of photodegradation in determining decomposition rate; which translated to 13% loss of leaf-litter C over the year for a scenario of a gap covering 20% of the forest floor. However, variation in C and nutrient dynamics during decomposition was not explored by Wang et al. (2021). To address this issue, the present study extended the previous study to examine the importance of solar radiation for lignin and N dynamics during the distinct seasons corresponding to changes in canopy phenology from spring to autumn in a temperate forest. We hypothesized that: (1) lignin loss would be greater where exposed to higher UV and short-wavelength visible light in the forest gap; (2) lignin loss would positively correlate with litter mass loss, modulated by spectral composition in the gap, but this spectral dependence would not be a significant factor in the understory because of its low solar irradiance for much of the year; (3) N would tend to be mineralized in the gap, because of

photodegradation driven by strong solar irradiance. On the other hand, in the understorey, N immobilization would dominate in the spring and early summer due to microbial activity during canopy flush, but dominance would switch to N release in late summer to autumn because of photofacilitation during leaf-fall.

2. Materials and methods

2.1. Study site

The experimental details were described in our previous study (Wang et al., 2021). Briefly, experimental plots were established in and around the Ogawa Forest Reserve (OFR, ca.100 ha) in the southern part of the Abukuma Mountain range in central Japan (36°56′N, 140°35′E, elevation 610 to 660 m above sea level). The reserve is an old-growth cool-temperate deciduous forest, dominated by *Quercus* spp., *Fagus* spp., *Acer* spp. (Masaki et al., 2002). The climate of OFR is characterized as humid with a mean annual temperature of 12.4 °C and annual precipitation of 1750 mm.

We set up a 50 × 50 m plot in the OFR understorey where the light environment was naturally impacted by seasonal canopy phenology, and a similar-size plot received full sunlight for nearly all hours in an unshaded gap (50 × 50 m size) created just outside the OFR *c* 5-km away, in order to investigate effects of solar spectral radiation on litter decomposition. Both plots had a similar slope aspect (south, 180°) and slope gradient (20°), and were protected by fences to exclude large mammals (mainly wild boar). The gap plot was clear-cut forest of similar composition to the understorey plot less than one year before the experiment in 2018. No plants grew on the ground which was covered by a natural litter layer from the beginning of experiment. Thus, it offered a homogeneous light environment and its proximity ensured a similar soil type and climate to the forest understorey plot.

2.2. Experimental manipulation and litterbox design

As described in Wang et al. (2021), we designed a field litter decomposition experiment comprising 12 litter species × 6 filter treatments × 2 plots × 4 collection times × 4 replicates, 2304 litterboxes in total. The litterboxes were an updated custom-made type based on our previous design (Pieristè et al., 2019). The dimensions of the litterbox were 18 cm wide × 21 cm long × 1.3 cm high, with a base made from sterile 2 mm mesh of the polyethylene fibre to avoid macrofaunal incursion while still allowing mesofauna access to the litter (referring to the effects of mesh size on mass loss from our previous study: Pieristè et al., 2019). Litterbox tops were made from a set of selected spectral film filters. The litterbox frame and central pillar were made of sterile plastic straws (21 cm long and 1.3 cm diameter, Bihin, Japan), in order to make a space in the litterbox to avoid contact between litter and the filters during decomposition. Holes of 2-mm diameter were drilled into the filter on a 1-cm grid in order to allow moisture, air, and microbes to interact with the litter within.

Six filter treatments were created: (*i*) Full-spectrum treatment, with a fully transparent polythene film (0.05 mm thick, 3904CF; Okura, Marugame, Japan), transmitting approximately 95% of the whole solar spectrum >280 nm; (*ii*) No-UV-B treatment, attenuating UV-B radiation <315 nm (0.125-mm-thick polyester film, Autostat CT5; Thermoplast, Helsinki, Finland); (*iii*) No-UV treatment, attenuating all UV radiation <400 nm (0.2-mm-thick Rosco E-Color 226 filter, Westlighting, Helsinki, Finland); (*iv*) No-UV/Blue treatment, attenuating all UV and blue wavelengths <500 nm (0.20-mm-thick Roscolux Supergel 312 filter); (*v*) No-UV/Blue–Green (BG) treatment, attenuating all UV radiation and BG wavelengths <580 nm (0.2-mm-thick Rosco E-Color 135 Deep Golden Amber filter), (*vi*) Dark treatment, attenuating all photosynthetically active radiation (PAR) and UV radiation (0.02-mm-thick polyethene film, white upper side and black lower side, Iwatani Materials Corp., Tokyo, Japan). The solar spectrum was measured in each litterbox under a clear sky at solar noon on 3rd June 2018 using a spectroradiometer (USR-45DA; USHIO, Tokyo, Japan) (Fig. 1a, Table S1).

2.3. Litter materials sampling and litterbox preparation

We selected 12 species with a range of trait values for variables, including litter N and lignin contents from different growth forms (trees, shrubs, herbaceous; Table 1). All litter samples were air-dried in a darkened room (25 °C, dehumidification mode of air conditioning) for one month. The leaf litter without petioles was placed flat inside newspapers and held in a wooden frame from December 25th, 2017 to January 20th, 2018, in order to maintain the litter flat. The pressed litter samples were kept in the dark at 25 °C and until their transfer to litterboxes.

A single-layer of non-overlapping litter was placed in the litterbox to make a homogeneous total surface area of litter (≈60% of the litterbox area), recorded by scanning each litterbox (EPSON scanner, GT-S600, Seiko, Nagoya, Japan). In the litterboxes, leaf litter was placed with the adaxial epidermis facing up, and fixed flat in position on the bottom mesh using stainless-steel staples (2–8 leaves per litterbox, weighing 0.2–1.0 g depending on the litter species), ensuring equivalent exposure to sunlight of all litter.

2.4. Litterbox deployment

Litterboxes were randomly pinned to the soil surface in four blocks within each plot (understorey and gap) on 18th April 2018 before canopy flush. Plots were checked every two weeks in order to keep litterboxes unobstructed, by removing any debris on the litterboxes and newly-grown plants. Hemispherical photographs were taken at 1.3-m height aboveground using a Nikon E4500 camera with a Sigma 8-mm fish-eye lens to capture canopy changes every month (Fig. 1b). Ambient UV-B, UV-A radiation, and PAR were continuously measured in the centre of plots at the ground level, integrated over 15-min intervals using two broadband UV-cosine sensors (UV-B and UV-A) (sglux GmbH, D-12489 Berlin, Germany) and a quantum sensor (LI-190SA; LI-COR, Lincoln, NE) respectively, recorded with a data-logger (LI-1400; LI-COR). UV-cosine sensors were calibrated by comparison with a traceable calibrated spectroradiometer Gigahertz BTS-2048-UV-S-F under natural sunlight clear sky conditions. The cumulative irradiance was calculated for each decomposition period (Fig. 1c). The spectral irradiance in litterboxes was checked during the experiment to ensure no changes occurred in the specified spectral attenuations of the filters, using a Maya 2000 Pro array spectrometer (Ocean Optics Inc., Florida, USA), recently calibrated for maximum sensitivity in the solar UV and PAR regions of the spectrum (Hartikainen et al., 2018). Litter temperature was measured at 30-min intervals by HOBO H8 Pro temperature loggers (Onset Computer Corporation, Bourne, Massachusetts, USA) placed under beech litter in one extra litterbox per filter type in each plot. Soil samples (to 5 cm depth) under three extra litterboxes per filter type were collected at solar noon once a month ($n = 3$ and a total of 18 soil moisture samples per plot). The gravimetric soil moisture content was calculated after oven drying (105 °C, 72 h).

2.5. Litterbox collection

Litterboxes were collected four times: 50, 110, 170, and 230 days after deployment (on June 7th, August 6th, October 5th, and December 4th, 2018), respectively timed to correspond with: canopy flush, completely closed canopy, canopy leaf-fall, and autumn canopy opening (see hemispherical photographs in Fig. 1b). Litterboxes were gently cleaned after retrieval and air-dried at the room temperature (dark, 25 °C) for one month. The ash-free (organic) mass and ash (inorganic) content were determined using a muffle oven (550 °C for 5 h). Four of 12 species were entirely collected before the final harvest, because they decomposed much faster than the rest. These species were two herbs, *Filipendula camtschatica* and *Pertya trilobata* and two shrubs, *Lindera obtusiloba* Blume and *Schisandra chinensis* (Table 1; Fig. S3).

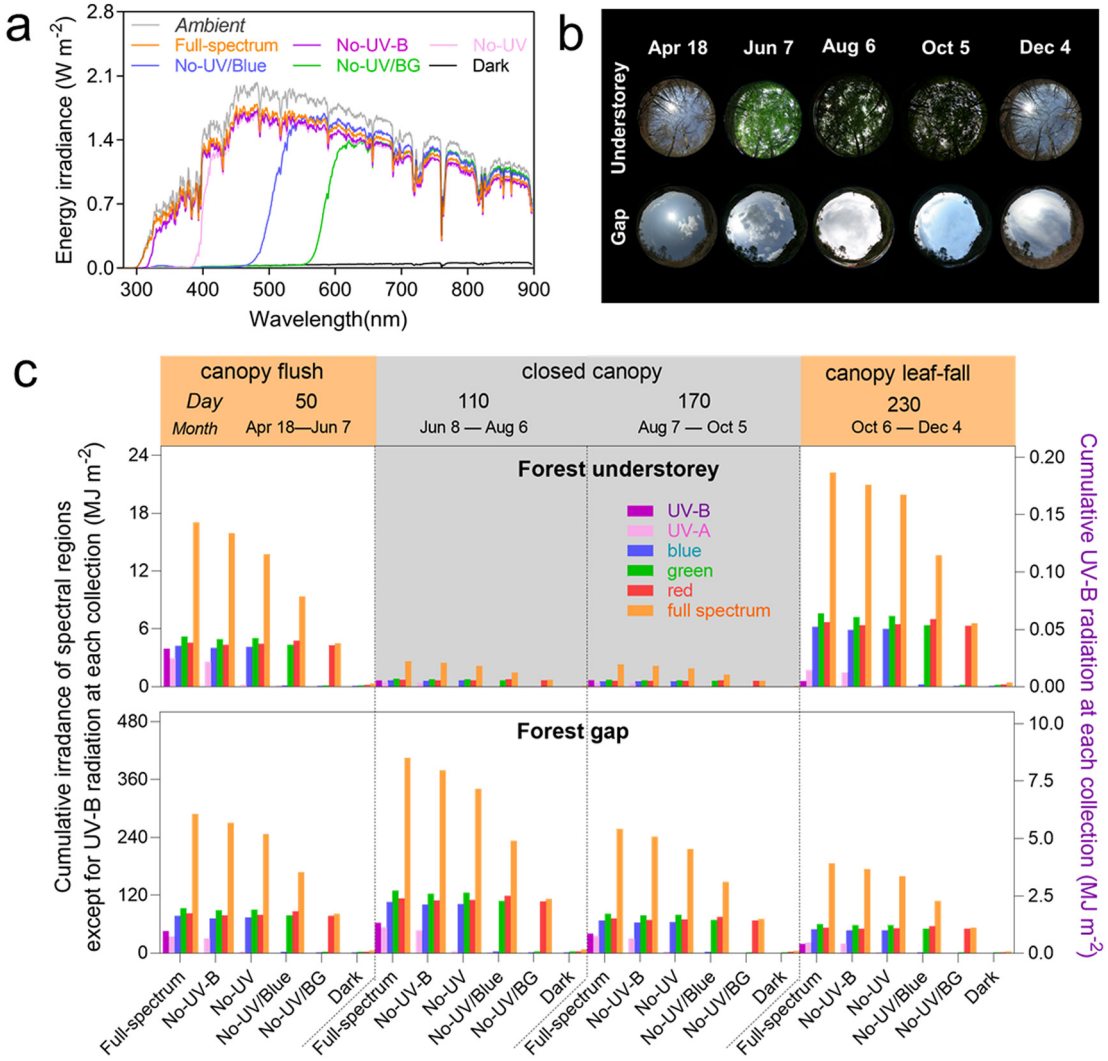

Fig. 1. Field experiment estimating the contribution of photodegradation to leaf-litter decomposition in a temperate deciduous forest through the seasons. (a) The attenuating filters used in custom-made litterboxes of different radiation treatments: [transmitting (*i*) >280 nm (full-spectrum); (*ii*) >315 nm (No-UV-B); (*iii*) >400 nm (No-UV); (*iv*) >500 nm (No-UV/blue); (*v*) >580 nm (No-UV/BG); (*vi*) no light (Dark)]. (b) Canopy hemispherical photographs of the experiment in the understorey and gap on four litterbox collection dates (April–December 2018), taken at 1.3 m aboveground using a Nikon E4500 camera with a Sigma 8-mm fish-eye lens. (c) Cumulative irradiance on litter in the understorey and gap over each of four decomposition periods. Litterboxes were collected four times: 50, 110, 170, and 230 days after deployment (on June 7th, August 6th, October 5th, and December 4th, 2018), respectively timed to correspond with: canopy flush, completely closed canopy, canopy leaf-fall, and autumn canopy opening.

2.6. Litter trait measurements

We measured initial leaf mass per area (LMA), nitrogen (N), carbon (C), and lignin concentrations of leaf litter prior to the start of the experiment (Table 1), and concentrations of the same chemicals from litter samples on each collection date. LMA was determined based on litter area and oven-dried weight of scanned leaves, using Fiji software (www.fiji.sc, ImageJ). The ground sample was also ashed at 550 °C for 5 h. N and C

Table 1
Species list and initial litter traits. Values are means (±SE) for each species (n = 5). Different letters across a column indicates significant difference ($P < 0.05$) among species, tested by Tukey's multiple comparison. C, carbon; N, nitrogen; LMA, leaf mass per area.

No. species	Family	Growth form	C (%)	N (%)	Lignin (%)	C:N	Lignin:N	LMA (gm^{-2})
S01 *Fallopia japonica*	*Polygonaceae*	*Herbs*	48.1 ± 0.47ab	1.9 ± 0.3a	16.9 ± 0.29ef	24.7 ± 0.43a	8.1 ± 0.13ef	95.3 ± 2.40a
S02 *Filipendula camtschatica*	*Rosaceae*	*Herbs*	42.8 ± 0.26f	1.7 ± 0.4b	12.4 ± 0.35 cd	25.2 ± 0.31a	7.3 ± 0.24c	35.1 ± 0.49f
S03 *Hosta sieboldiana*	*Asparagaceae*	*Herbs*	45.8 ± 0.76cde	0.7 ± 0.1e	11.3 ± 0.12bc	63.9 ± 1.60f	15.8 ± 0.53de	63.5 ± 1.15c
S04 *Pertya trilobata*	*Asteraceae*	*Herbs*	42.8 ± 0.15f	1.5 ± 0.1c	11.5 ± 0.10d	29.1 ± 0.49bc	8.6 ± 0.18c	33.7 ± 0.69f
S05 *Lespedeza bicolor Turcz. var. bicolor.*	*Fabaceae*	*Shurbs*	46.8 ± 0.30bcd	1.4 ± 0.2c	16.6 ± 0.16f	32.7 ± 0.91d	11.5 ± 0.22 cd	44.1 ± 0.95e
S06 *Lindera obtusiloba Blume*	*Lauraceae*	*Shurbs*	45.4 ± 0.26de	0.7 ± 0.2e	11.3 ± 0.19b	61.8 ± 3.31f	15.2 ± 0.85a	31.6 ± 0.78 g
S07 *Schisandra chinensis*	*Schisandraceae*	*Shurbs*	40.5 ± 0.12 g	1.5 ± 0.1c	7.8 ± 0.11a	27.8 ± 0.12b	6.6 ± 0.07bc	24.8 ± 0.43 h
S08 *Vitis coignetiae*	*Vitaceae*	*Shurbs*	45.1 ± 0.22de	1.5 ± 0.6c	12.6 ± 0.61e	30.6 ± 0.57 cd	9.9 ± 0.52b	70.6 ± 1.82b
S09 *Acer carpinifolium*	*Sapindaceae*	*Trees*	44.8 ± 0.31e	1.4 ± 0.6c	21.3 ± 0.59 g	32.4 ± 0.65d	15.6 ± 0.36 g	42.3 ± 1.00e
S10 *Betula platyphylla*	*Betulaceae*	*Trees*	48.7 ± 0.46a	1.1 ± 0.1d	16.4 ± 0.06f	45.8 ± 0.64e	15.3 ± 0.29 h	72.9 ± 1.11b
S11 *Fagus crenata Blume*	*Fagaceae*	*Trees*	48.4 ± 0.22ab	0.9 ± 0.3e	23.0 ± 0.26 g	57.1 ± 2.40f	24.8 ± 0.90f	50.3 ± 0.92d
S12 *Quercus crispula Blume*	*Fagaceae*	*Trees*	47.4 ± 0.41abc	0.8 ± 0.4e	15.7 ± 0.38f	58.3 ± 1.93f	20.0 ± 0.50 fg	74.9 ± 1.80b

concentrations were determined using an elemental analyser (the precision <0.1%, Vario MAX cube, Hanau, Germany) with acetanilide as the standard. An improved acetyl-bromide procedure (Iiyama and Wallis, 1990) was used to determine the lignin content, and calculated from the fitted calibration curve (Fukushima and Hatfield, 2001).

2.7. Calculation and statistical analyses

Ash content was used for correction to obtain ash-free dry weight for litter mass and chemical contents (C, N, and lignin). For the main analysis, all litter types were pooled and each species (using its mean value) was treated as a replicate, because we were interested in the general pattern rather than species specific response of a litter type. We calculated the percentage mass remaining ratio (M) and chemical contents (Q) per unit of mass over each period of the experiment using the following equations;

$$M = X^t / X^0 * 100\% \quad (1)$$

$$Q = (X_t \cdot Y_t)/(X_0 \cdot Y_0) * 100\% \quad (2)$$

where X_0, X_t, and Y_0, Y_t are dry mass and chemical concentration at the beginning of the experiment and at time t, respectively. The loss rates were calculated by subtracting M from 100%.

To examine the difference in mass loss and patterns of variation in mass loss among decomposition periods, we calculated relative mass loss ratio fractions (F) of litter C, N, and lignin during each period compared with initial litter (the difference between two ratios of remaining mass divided by the time interval), instead of the absolute values (simply the difference between two masses divided by the time interval). Due to the unequal lengths of each period, F was calculated with the following equation to exclude the time effect,

$$F = (Q_{t-1} - Q_t)/\Delta T \quad (3)$$

where Q_t, Q_{t-1} are the ratio of mass remaining at time t and the previous time ($t - 1$), respectively. ΔT is the difference in the length duration (numbers of days) between the two collection times.

We used one-way ANOVA to analyze differences in initial traits of leaf litter among 12 species, and linear mixed-effects models (LMM) to test the effects of three fixed factors, canopy structure (understorey and gap), season, and filter treatment and their interactions on the loss of chemical content, litter quality (C:N and lignin:N), and loss fractions, with species as the random factor. Differences between canopy structure, and among treatments, were tested by Tukey's multiple comparison. To assess the effects of specific spectral regions on the dry-mass loss, chemical content, and litter quality, we did a one-way ANOVA with pairwise contrasts (function glht, R package multcomp, (Hothorn et al., 2008)) at each collection time (referring to our previous studies: Pieristè et al., 2019; Wang et al., 2021). We used Benjamini-Hochbergs (BH) method (Benjamini and Hochberg, 1995) to correct these P values for multiple comparisons. Two-way ANOVA was used to test the effects of canopy structure and filter treatment on soil moisture content.

To quantify the relative effect of photodegradation, we calculated the spectral response ratios (RR) of dry mass and lignin loss between spectral contrasts (Day et al., 2015). We also calculated RR of mass loss in our previous study (Wang et al., 2021), but in the present study lignin fraction increased (negative loss ratios) rather than consistently decreasing over the experiment period. Thus, here we modified the response ratio calculation according to the equation,

$$RR = (Q_i - Q_j)/|Q_j| \quad (4)$$

where Q is the loss ratio (X_t / X_0) at time t, and i and j are two treatments of a contrast comparison. As the RR value (e.g. $RR_{UV\text{-}B}$) increases above 0, more mass or lignin is lost from litter, due to a specific spectral region, e.g. UV-B radiation, compared with litter that did not receive UV-B radiation. The effects of three fixed factors (time, canopy structure, and filter treatment) and their interactions on RR were analyzed by LMM as above.

We further used ordinary least squares regression (OLSR) to assess the relationships between response ratios of mass and lignin loss. We tested differences in slopes among treatments with nonlinear extra sum-of-squares F test. Yeo-Johnson power transformation was used to ensure normality (Yeo and Johnson, 2000). All statistical analyses were done in R version 3.6.3 (R Core Team 2020).

3. Results

3.1. Litter microclimate

Accumulated solar spectral irradiance over the experimental period was lower in the forest understorey than in the gap (Figs. 1b,c, S1). Understorey solar spectral irradiance fluctuated greatly over the collection periods, modified by canopy phenology. In the understorey during canopy closure, PAR, blue light, UV-A, and UV-B radiation were attenuated by the canopy by up to 96.1%, 96.0%, 96.3% and 98.6%, respectively, (Fig. S1). In the understorey, cumulative irradiance on litter over the experimental period was drastically reduced when the canopy was closed during the 2nd and 3rd experimental periods (from June to August, and from August to October), and irradiance was only 5.9 % and 6.7 % of that accumulated in the understorey respectively during each period (Fig. 1c). Soil moisture content varied insignificantly among filter treatments and between the understorey and gap (Fig. S2a). The litter temperature was similar among filter treatments within the plot, but in the gap it was higher (22.4 °C) than in the understorey (16.7 °C) (Fig. S2b).

3.2. Impacts of solar radiation on C, N, and lignin contents during litter decomposition

Alongside the effect on mass loss and decay rate described in Wang et al., 2021, litter quality, in terms of C, N and lignin during leaf litter decomposition, was significantly affected by canopy structure, filter treatment, season and their interactions (Table 2). During the 1st decomposition period, C loss in the understorey was 15 % under the full spectrum of sunlight, where UV-B radiation (Full-spectrum vs. No-UV-B treatment)

Table 2
Linear Mixed-Effects Models (LMM) results for three fixed factors (canopy structure, filter treatment, and season) and their interactions on loss of carbon [C], nitrogen [N], lignin, C:N, and lignin:N with species as the random factor. Bold indicate statistically significant.

Factors	df	C loss (%)		N loss (%)		Lignin loss (%)		C:N		Lignin:N	
		F	*P*	*F*	*P*	*F*	*P*	*F*	*P*	*F*	*P*
Canopy structure (CS)	1	**322.66**	**<0.001**	**435.86**	**<0.001**	**79.58**	**<0.001**	**62.33**	**<0.001**	**264.57**	**<0.001**
Filter treatment (FT)	5	**116.78**	**<0.001**	**60.82**	**<0.001**	**82.62**	**<0.001**	2.07	0.067	0.57	0.722
Season (S)	1	**4465.30**	**<0.001**	**313.74**	**<0.001**	**723.08**	**<0.001**	**1680.60**	**<0.001**	**49.44**	**<0.001**
CS × FT	5	**111.78**	**<0.001**	**45.93**	**<0.001**	**70.19**	**<0.001**	**2.60**	**0.024**	0.15	0.979
CS × S	1	0.20	0.655	0.00	0.962	**6.85**	**0.009**	**4.32**	**0.038**	**4.53**	**0.033**
FT × S	5	**7.19**	**<0.001**	**7.35**	**<0.001**	**4.33**	**0.001**	0.93	0.458	1.41	0.216
CS × FT × S	5	**16.63**	**<0.001**	**9.79**	**<0.001**	**9.39**	**<0.001**	**4.19**	**0.001**	**6.44**	**<0.001**

contributed 80 % of this C loss (the estimated effect of UV-B, $P < 0.001$, Fig. 2a). However, the differences in filter treatments progressively declined with canopy phenology (i.e., as the canopy closed) and were absent by the last period before collection (by days 170 and 230) (Table S2). In contrast, C loss in the gap was up to 75 % under the full spectrum treatment, and blue light contributed 27 % to the C loss attributable to photodegradation over the whole study period (Fig. 2a).

Understorey litter N content increased during the 1st and 2nd decomposition periods and was significantly enhanced by red light and UV-A radiation, respectively in the 1st and 2nd period (Figs. 2b, S4). In the forest gap, N loss was significantly higher in treatments exposed to UV-B radiation and blue light during the 3rd and 4th periods (Fig. 2b, Table S3). In terms of lignin dynamics, there were no significant spectral effects on lignin in the understorey during canopy flush, while exposure to the full spectrum of sunlight enhanced litter lignin loss by 64 % in the gap compared with darkness, and blue light contributed 42 % to the effect of photodegradation on lignin over the whole study period (Figs. 2c, S5; Table S4). The C:N and lignin:N ratios were not significantly affected by filter treatment, but were affected by the interaction of filter treatment with canopy structure and season (Fig. S6; Table 2, S5,6), both of which greatly impacted the cumulative amount of solar radiation reaching the litter surface (Fig. 1).

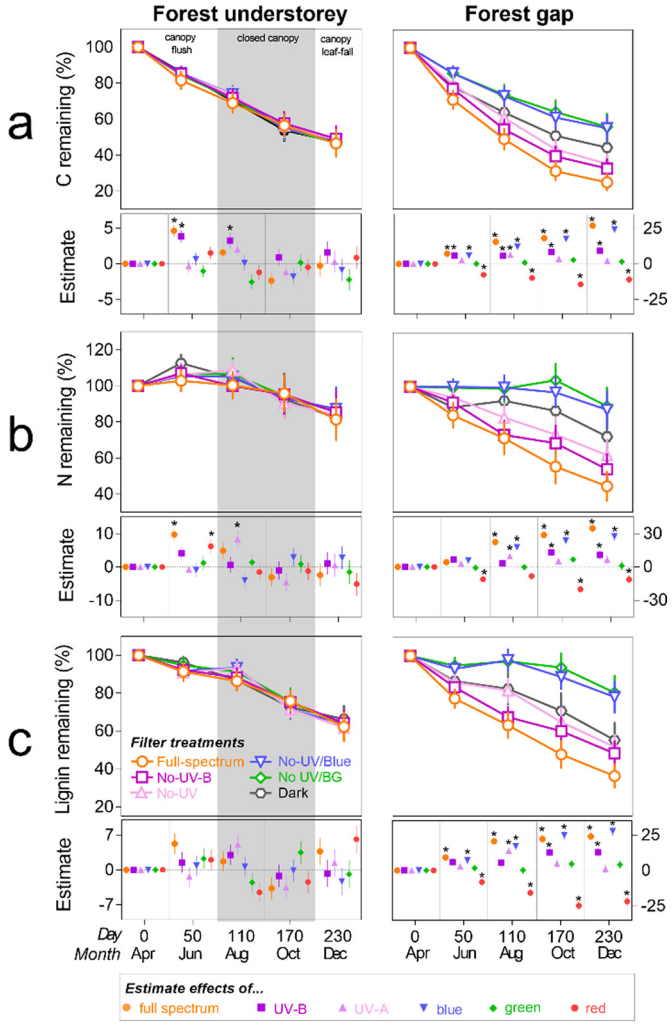

Fig. 2. Seasonal variation in carbon, nitrogen and lignin loss from litter in response to solar spectral regions in the forest understorey and canopy gap. Carbon (C) loss (a), nitrogen (N) loss (b), and lignin loss (c) in leaf litter from 12 species (pooled) exposed to solar radiation in six filter treatments in the understorey and gap. At the bottom of each figure, estimates represent pairwise comparison results for ratios responding to filter treatments: *F*-tests, with the Benjamini-Hochberg (BH)'s correction for multiple comparisons, were used to calculate the *P* values. Each point represents effects of spectral regions by comparing contrasts between treatments. Full-spectrum treatment vs Dark treatment, Full-spectrum treatment vs No-UV-B treatment, No-UV-B treatment vs No-UV treatment, No-UV treatment vs No-UV/Blue treatment, No-UV/Blue treatment vs No-UV/Blue-Green (BG), No-UV/ BG treatment vs Dark treatment, give the effect of full spectrum, UV-B, UV-A, blue, green, and red light, respectively. The asterisk indicates the significant difference between treatments. Details are shown in Table S4–6. Values are means across species (±SEM, $n = 12$). Four fast-decomposing species were totally collected at the third time-point (October) (Fig. S3), and these data at the final collection, calculated according to the decay rates (k) of these species, was interpolated in the curves.

3.3. Impact of solar radiation on C, N and lignin fractions during litter decomposition

The C fraction lost was significantly affected by filter treatment and season; such effects interacted significantly with canopy structure (Table 3). In the forest gap, the C fraction lost in treatments exposed to the full spectrum of sunlight dramatically decreased from April to December (from 0.58 % to 0.11 % day^{-1}) (Fig. 3a). In particular, a larger C fraction was lost from litter exposed to UV radiation and blue light during the 1st and 2nd periods, while the C fraction lost tended to converge among filter treatments at the end of the experiment. In the understorey, the C fraction lost was evident in treatments exposed to UV-B radiation during the 1st periods, but during the 3rd period, it became greater in treatments attenuating UV radiation and blue light than the others (Fig 3a).

The temporal effect on N fraction lost significantly varied according to canopy structure (CS × S interaction: $P < 0.001$, Table 3). In the gap, litter N fraction lost was constantly higher in the full-spectrum treatment than the No-UV/Blue and No-UV/BG treatments by the 3rd period, however this difference was no longer apparent at the end of the experiment (Fig. 3b). In the understorey, the N fraction actually increased during canopy flushing (i.e., N was gained) but N was lost from the 2nd period with the highest values for N fraction lost found during the 3rd period towards canopy leaf-fall (Fig. 3b). This suggests N immobilization took place during the early phases, and N release at the later stages, of the decomposition process.

The effect of season and filter treatments on lignin fraction lost changed significantly depending on canopy structure (Table 3). Lignin loss varied in a similar pattern to the fractional N loss irrespective of season, treatments, and canopy structure (Fig. 3c), with one exception; that lignin loss was not lower but higher during the 1st period in comparison with the 2nd period of decomposition in the understorey. Regarding the target of photodegradation, in the understorey *RR*(lignin loss) was positively correlated with *RR*(mass loss) irrespective of the spectral region considered ($F = 0.30$, $P = 0.91$, Table 4, Fig. 4a), whereas in the gap the sign and strength this relationship varied significantly depending on the spectral region considered ($F = 4.44$, $P < 0.001$, Table 4, Fig. 4b).

Table 3
Linear Mixed-Effects Models (LMM) results for three fixed factors (canopy structure, filter treatment and season) and their interactions on period loss fractions (% day^{-1}) of carbon [C], nitrogen [N] and lignin with species as the random factor. Bold indicate statistically significant.

Factors	df	C loss fraction		N loss fraction		Lignin loss fraction	
		F	*P*	*F*	*P*	*F*	*P*
Canopy structure (CS)	1	2.17	0.141	**9.19**	**0.003**	0.59	0.445
Filter treatment (FT)	5	**3.46**	**0.004**	2.09	0.065	**2.32**	**0.042**
Season (S)	1	**81.16**	**<0.001**	**65.08**	**<0.001**	**20.15**	**<0.001**
CS × FT	5	**4.33**	**0.001**	1.72	0.128	**2.25**	**0.048**
CS × S	1	**15.78**	**<0.001**	**19.22**	**0.001**	**5.44**	**0.020**
FT × S	5	1.46	0.200	0.68	0.637	1.84	0.104
CS × FT × S	5	1.08	0.373	0.33	0.893	0.84	0.524

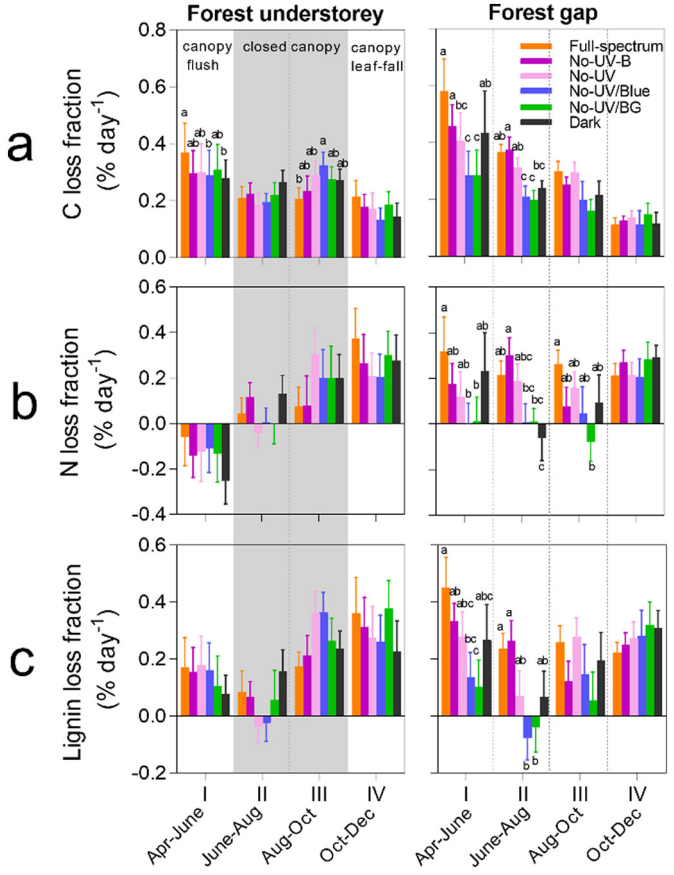

Fig. 3. The carbon, nitrogen and lignin loss ratio fraction in six filter treatments at each of four decomposition periods in the forest understorey and canopy gap. Carbon (C) loss (a), nitrogen (N) loss (b), and lignin loss (c) in leaf litter from 12 species (pooled). Bars are means across species (±SEM, $n = 12$). Different lowercase letters denote significant difference among spectral regions within a period ($P < 0.05$).

4. Discussion

4.1. The importance of photodegradation in accelerating C loss in temperate forest ecosystems depends on both canopy structure and canopy phenology

The divergence among C loss curves highlights the different effects of filter treatments in the forest gap (Fig. 2a), and illustrates how photodegradation significantly accelerates surface litter decomposition where gaps open in the forest canopy (Fig. 2a). This is consistent with findings from drylands (Austin and Vivanco, 2006; Austin et al., 2016; Berenstecher et al., 2020), in suggesting photodegradation can be a major contributor to C turnover across terrestrial ecosystems including temperate forests (Wang et al., 2021).

In the understorey, C loss curves across filter treatments tended to be convergent (Fig. 2a), which implies that microbial decomposition rather than photodegradation drives litter mass loss in the understorey where solar irradiance is low (Fig. 1). As well as reducing irradiance, forest canopy shade can decrease the daytime temperature and evaporation from the soil, potentially accelerating decay by maintaining a cool and humid environment on the forest floor. The favorable environment for decomposition meant that the average C lost by litter across all treatments in the understorey was not much less than that in the gap (Fig. 2a), where temperature and evaporation are higher during the daytime (Fig. S2b). This result is consistent with findings from various biomes regarding canopy-cover effects, e.g., in tropical (Marinho et al., 2020), subtropical (Ma et al., 2017), and temperate forests (Wallace et al., 2018). Nevertheless, we found evidence that photodegradation driven by UV-B radiation before canopy closure does function in the understorey (Fig. 2a). After the spring canopy-flush, most sunlight is absorbed by leaves in the canopy, especially blue and red light which are important in photosythesis (Navrátil et al., 2007). Whereas, before canopy closure in spring, UV-B and UV-A radiation and blue light are relatively enriched in the diffuse radiation of understorey shade compared to longer wavelengths, mainly because of their greater Rayleigh scattering by atmosphere (Durand et al., 2021; Flint and Caldwell, 1998; Hartikainen et al., 2018).

The importance of UV-B radiation in our findings differs from previous studies which emphasized the importance of UV-A and blue light in understorey decomposition (Pieristè et al., 2019). The reason for this difference may be the higher relative contribution of UV-B radiation to the spectrum in our study, because it was performed at a lower latitude in Ibaraki Japan compared with Rouen or Helsinki where the low solar elevation angle means that UV-B irradiances are low at the time of canopy closure.

Table 4
Ordinary least squares regression (OLSR) results for relationships between the response ratio of *RR*(mass loss) and *RR*(lignin loss) among spectral regions under two canopy structure over the whole experimental period. $n = 44$ from 12 species and 4 collection times, except for two herb species (*Filipendula camtschatica* and *Pertya trilobata*) and two shrub species (*Lindera obtusiloba* Blume and *Schisandra chinensis*) were totally collected at the third time (October), due to their fast decomposition rate. P_1-values in bold indicate that the regression was statistically significant ($P < 0.05$). Difference in slopes among spectral regions was tested with nonlinear extra sum-of-squares *F*. P_2-values in bold indicate that the slopes were significantly different among relationships. Bold indicate statistically significant.

Spectral regions	Forest understorey				Forest gap			
	Slope	Intercept	R^2	P_1	Slope	Intercept	R^2	P_1
Full spectrum	0.45	−0.16	0.31	**<0.001**	0.87	0.45	0.51	**<0.001**
UV-B	0.51	0.26	0.36	**<0.001**	0.23	0.35	0.17	**0.006**
UV-A	0.53	−0.16	0.42	**<0.001**	0.37	0.20	0.23	**0.001**
Blue	0.42	−0.26	0.28	**<0.001**	0.52	0.66	0.26	**0.000**
Green	0.40	−0.42	0.33	**<0.001**	0.39	0.01	0.23	**0.001**
Red	0.39	−0.19	0.26	**<0.001**	0.21	−1.03	0.08	0.059
F	0.30				4.44			
P_2	0.91				**0.00**			

4.2. Lignin decomposition dynamics depends on spectral composition and canopy structure

The dynamics of lignin loss was driven by blue light in the forest gap, particularly at the early stages of decomposition (Figs. 2c, 3c). Lignin is generally considered to be a "bottleneck" for C turnover (Austin et al., 2016), since it is not only recalcitrant to enzymatic degradation (Swift et al., 1979), but also provides limited labile C compounds to microbes (Manzoni et al., 2008), being largely decomposed by fungi during the later phases of decomposition (Osono and Takeda, 2001). On the other hand, lignin is subject to photodegradation, due to its effective absorption of UV radiation and short-wavelength visible light (Austin and Ballaré, 2010). Our finding of respectively higher and lower lignin loss when UV radiation and blue-green light were transmitted and attenuated in the forest gap, is the first to show the dual role of lignin is not limited to drylands, but is also valid for mesic ecosystems where solar irradiance reaches on the litter surface. Austin et al. (2016) found that photodegradation via blue-green light mainly alleviated the bottleneck imposed by lignin in cell walls and enhanced subsequent microbial decomposition, highlighting the importance of photofacilitation from solar radiation. However, our in situ study provides evidence that ambient sunlight can directly drive lignin loss in the field, modulated by spectral composition (Fig. 4b).

Both photochemical mineralization and photofacilitation may underpin the reported effect on lignin decomposition, though it is difficult to disentangle these two mechanisms in the field as both occur simultaneously. In mesic ecosystems, a precipitation pulse occurs much more frequently than in arid and semi-arid ecosystems (Song et al., 2011). Hence, many small molecules and soluble compounds locked within the cell walls are

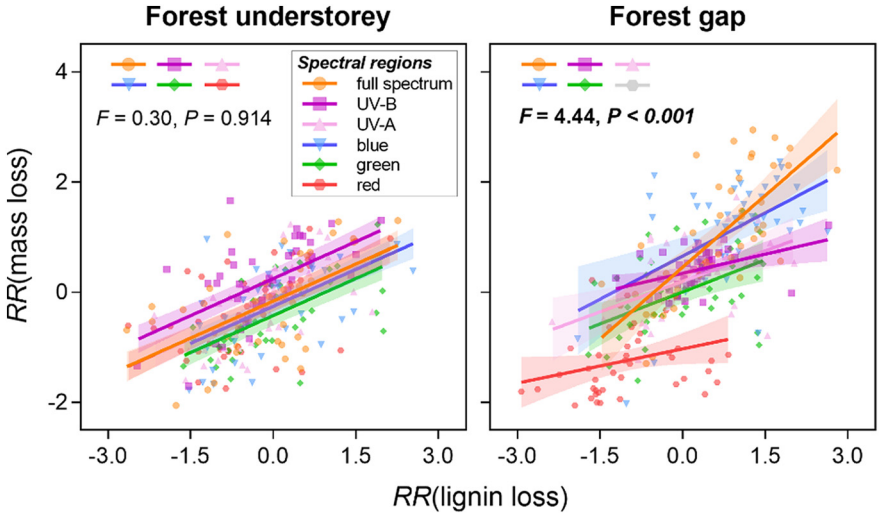

Fig. 4. Relationships between the response ratios of *RR*(mass loss) and *RR*(lignin loss) among spectral regions in the forest understorey and canopy gap over the whole decomposition period (April–December 2018). The lines of best fit using ordinary least squares regression (OLSR) are plotted. Symbols associated with solid colored lines in each figure denote significant relationships ($P < 0.05$). $n = 44$ from 12 species and 4 collection times, except for two herb species (*Filipendula camtschatica* and *Pertya trilobata*) and two shrub species (*Lindera obtusiloba* Blume and *Schisandra chinensis*) which were totally collected at the third time point (October), due to their fast decomposition rate. Detailed regression results are shown in Table 4. *F* and *P* values represent the difference in slopes among spectral regions tested with nonlinear extra sum-of-squares *F* test, and values in bold indicate statistically significant differences ($P < 0.05$).

easily leached out in moist conditions once the lignin linkages are broken down by photochemical mineralization. Meanwhile, gas emissions may be responsible for a considerable fraction of litter mass loss. For instance, dryland studies found that CO_2 emission from direct photochemical mineralization accounted for as much as 39% of the C loss through photodegradation (Day and Bliss, 2019, 2020), without it ever entering the soil C pool (Méndez et al., 2019). Although gas emissions were not directly quantified in the present study, scaling up to the ecosystem level, we modeled the contribution of photodegradation to litter C loss, finding it to contribute between 13 and 63 % compared with typical estimates of litter decomposition in the understorey (Wang et al., 2021). This contribution may partly explain the missing C loss in global carbon budgets (Neale et al., 2021) for mesic ecosystems, which to date is unaccounted for.

More lignin was lost in the understorey when exposed to UV radiation and blue light during our first and final collection periods; those characterized by an open canopy (Fig. 3c). On the contrary, the lignin loss fraction was slightly higher in treatments attenuating UV and blue light during canopy closure (August–October), despite the irradiance then being low. This finding is in agreement with our previous reports that fungi are favored by the exclusion of UV, blue and green light (Pancotto et al., 2003; Pieristè et al., 2020a). This is cogent with the suggestion that microbial degradation plays a key role in litter decomposition processes in shady, cool, and humid environments (Figs. S1, 2), which are particularly favorable to microbial activities (Ma et al., 2017). In the forest gap more C, N and lignin were lost in the darkness (Fig. 2); a result which could similarly be ascribed to high microbial degradation (Pieristè et al., 2020a; Wang et al., 2020).

4.3. N tends to be mineralized in the forest gap but immobilized in the understorey during litter decomposition processes

Similar to lignin loss, N was quickly lost from litter in Full-spectrum, No-UVB, and No-UV treatments in the forest gap (Fig. 2b). Differences in the respective fraction of N loss (Fig. 3b) indicated that UV radiation and blue light generally increased N mineralization. This implies that high solar irradiance promotes nutrient release from litter through lignin photochemical mineralization (Austin et al., 2016; Méndez et al., 2019). As a consequence, the release dynamics of N and C and lignin appear to be coordinated in the gap, as supported by convergent C:N and lignin:N ratios among treatments (Fig. S6). Moreover, UV radiation and blue light may also inhibit microbial activitiy and reduce N immobilization (Gallo et al., 2006; Barnes et al., 2015; Pieristè et al., 2020a), though it is not clear how photoinhibition counterbalances photofacilitation in mesic ecosystems. We found that N release in the gap was continuous over the experimental period (Fig. 2b), rather than occurring mostly during the early stages of decomposition as previously reported from a controlled experiment with dryland litter-soil (Foereid et al., 2010). A possible explanation for this difference in findings between biomes could be that solar radiation disrupts cell-wall integrety in litter especially when combined with changes in local weather (e.g. temperature or rainfall fluctuations) in a mesic climate.

On the other hand, N in the understorey was immobilized during canopy flush but switched to N release in late summer prior to canopy leaf-fall (Figs. 2b, 3b). In general, N immobilization can be attributed to microbial activity on the litter surface (Parton et al., 2007). During the early phase of decomposition, microbes, particularly bacteria, may be facilitated by the presence of micromolecules (Parton et al., 2007). These may be produced in part by direct photomineralization before canopy closure (Baker and Allison, 2015; Pieristè et al., 2020a), as suggested by the high C loss fraction corresponding to loss of the low lignin fraction (Fig. 3). Under an environmental scenario with increased N deposition, we could expect the initial C:N ratio of litter to be lower which might affect the decomposition rate in a similar manner to that following increase in N immobilization during the early phase of decomposition (Sun et al., 2016). Hereafter, the fractions of N and lignin loss were small between June and August, whereas the C loss fraction remained large. This may imply high initial microbial activity consuming C available as labile cell solutes (Lin and King, 2014), and suggests that photofacilitation (or photopriming) lags after canopy flushing. During later phases of decomposition, high N release may not only be related to increased penetration of solar irradiance through the canopy during and after leaf-fall, but also associated with the lower C:N ratios of litter (Fig. S6a), due to N accumulation during the preceding period. Furthermore, relatively high photodegradation responding to UV-B radiation (Fig. S7a) suggests that varying understorey UV-B radiation may have a positive effect on microbes via photofacilitation outweighing its negative effect of photoinhibition. This supports the hypothesis that dark periods are essential for photopriming over a daily timescale (Lin et al., 2018), or even within a single day (Gliksman et al., 2017), e.g., under the fluctuating

light conditions found in the forest understorey, whereby litter in shade may receive very little irradiance until caught in a sunfleck.

Variations in N mineralization, immobilization and release, driven by photodegradation during decomposition, may affect seasonal changes in nutrient availability in forest soils for plants and microbial communities that are partially mediated by the phases of canopy phenology. The magnitude of these fluctuations in N dynamics will also depend on global changes, such as stratospheric ozone and climate (e.g., cloud cover) which modify incoming solar radiation (Sulzberger et al., 2019), on regional and local scales. This means that soil nutrient availability may be underestimated based on traditional models of N dynamics during decomposition, which fail to account for the role of photodegradation in the time-course release of N from litter. However, caution is required in assessing the relationship between N dynamics and canopy phenology resulting from this experiment, since litter decomposition in temperate deciduous forests starts in autumn and we began our experiment in spring. Although the N dynamics we observed are similar to the general pattern found in experiments starting in autumn (i.e., N immobilization in early stage of decomposition, and N release in later stage of decomposition) (Pei et al., 2019), absolute microbial activities may differ between winter and spring. Future studies are necessary to understand microbial mechanisms that interact seasonally with photodegradation.

The flat single-layer litterbox was designed to ensured homogeneous exposure to sunlight, avoiding litter overlapping in the traditional litterbag (Pieristè et al., 2019, 2020a; Wang et al., 2021). However, this could produce an overestimate the effect of solar radiation on litter turnover in temperate forests, where the leaf-litter layer is generally thick. Nevertheless, photodegradation on the surface layer may have potential priming effects on litter decomposition, since the leaf-fall timing is different among species. It may consequently promote litter turnover after being covered by new litter.

5. Conclusions

The present study demonstrates that canopy structure and phenology can modulate the impacts of solar radiation on C and N dynamics during leaf litter decomposition in a temperate forest. Lignin loss was greater and significantly correlated with mass loss due to solar radiation in the forest gap, where it is exposed to higher solar irradiance, particularly blue light. Whereas in the understorey, UV-B radiation made the greatest contribution to photodegradation, which was only a factor affecting decomposition before spring canopy closure. On the other hand, periodic C and lignin loss fractions were decoupled from cumulative irradiance during canopy closure. Similarly, N tended to be mineralized in the gap during lignin decomposition, while in the understorey was immobilized during canopy flush but by late summer N release had become the dominant process. Our findings highlight the need to incorporate photodegradation into empirical models predicting how global C and nutrient cycles respond to climate changes. This is required because of large spatiotemporal changes in photodegradation and its interaction with land use and disturbance.

CRediT authorship contribution statement

Qing-Wei Wang, **Hiroko Kurokawa**, and **Thomas Matthew Robson**: Experimental design. **Qing-Wei Wang**, **Marta Pieristè**, and **Thomas Matthew Robson**: Field measurement. **Qing-Wei Wang**: field management, litterbox collection, lab determination, data analysis, writing. All: Reviewing and Editing.

QWW, **HK**, and **TMR** conceived and designed the experiment. **QWW** and **TK** collected leaf litter. **QWW**, **TMR**, and **MP** measured spectrum of field light environments and litterboxes. **QWW** and **HK** set up the field decomposition experiment. **QWW** managed and retrieved litterboxes, and determined ash-free mass loss and litter traits. **QWW** did statistical analysis and wrote the draft of the manuscript, and the remaining coauthors did the revision.

Declaration of competing interest

The authors declare that they have no known competing financial interests or personal relationships that could have appeared to influence the work reported in this paper.

Acknowledgments

We thank Drs. Qingmin Han, Masatake Araki, Jun Hidema for equipment support, Drs. Mitsue Shibata and Tamotsu Sato for facilities at FFPRI, Nobuko Hirai, Masako Hosoi, Yasuko Ogane, Hiroko Shiomi, and Rie Takaya for their helps of laboratory work, and arboretum and nursery managers for their helps of field work. Q.-W Wang is grateful to the Japan Society for the Promotion of Science (JSPS), Japan for awarding of JSPS Post-doctoral Research Fellowship for Foreign Researchers in Japan (FY 2017-2019). This research was funded by the National Natural Science Foundation of China (NSFC) (32122059), the Chinese Academy of Sciences Young Talents Program, and LiaoNing Revitalization Talents Program (XLYC2007016) to QWW, by the Japan Society for the Promotion of Science (KAKENHI, 17F17403) and Chinese Academy of Sciences President's International Fellowship Initiative (2022VCA0010) to QWW and HK, by Academy of Finland decisions #266523, #304519 and #324555 to TMR, personal EF project and a grant from the Region “Haute-Normandie” through the GRR-TERA SCALE (UFOSE Project) to MP, and WMZ by NSFC (41977423, 41877549).

Appendix A. Supplementary data

Supplementary data to this article can be found online at https://doi.org/10.1016/j.scitotenv.2022.153185.

References

Adair, E.C., Parton, W.J., King, J.Y., Brandt, L.A., Lin, Y., 2017. Accounting for photodegradation dramatically improves prediction of carbon losses in dryland systems. Ecosphere 8, e01892.

Almagro, M., Maestre, F.T., Martínez-López, J., Valencia, E., Rey, A., 2015. Climate change may reduce litter decomposition while enhancing the contribution of photodegradation in dry perennial Mediterranean grasslands. Soil Biol. Biochem. 90, 214–223.

Asao, S., Parton, W.J., Chen, M.S., Gao, W., 2018. Photodegradation accelerates ecosystem N cycling in a simulated California grassland. Ecosphere 9, e02370.

Augspurger, C., Cheeseman, J., Salk, C., 2005. Light gains and physiological capacity of understorey woody plants during phenological avoidance of canopy shade. Funct. Ecol. 19, 537–546.

Austin, A.T., Ballaré, C.L., 2010. Dual role of lignin in plant litter decomposition in terrestrial ecosystems. Proc. Natl. Acad. Sci. U. S. A. 107, 4618–4622.

Austin, A.T., Méndez, M.S., Ballaré, C.L., 2016. Photodegradation alleviates the lignin bottleneck for carbon turnover in terrestrial ecosystems. Proc. Natl. Acad. Sci. U. S. A. 113, 4392–4397.

Austin, A.T., Vivanco, L., 2006. Plant litter decomposition in a semi-arid ecosystem controlled by photodegradation. Nature 442, 555–558.

Baker, N.R., Allison, S.D., 2015. Ultraviolet photodegradation facilitates microbial litter decomposition in a Mediterranean climate. Ecology 96, 1994–2003.

Baldocchi, D.D., Matt, D.R., Hutchison, B.A., McMillen, R.T., 1984. Solar radiation within an oak—Hickory forest: an evaluation of the extinction coefficients for several radiation components during fully-leafed and leafless periods. Agric. For. Meteorol. 32, 307–322.

Ball, B.A., Christman, M.P., Hall, S.J., 2019. Nutrient dynamics during photodegradation of plant litter in the Sonoran Desert. J. Arid Environ. 160, 1–10.

Barnes, P.W., Throop, H.L., Archer, S.R., Breshears, D.D., McCulley, R.L., Tobler, M.A., 2015. Sunlight and soil–litter mixing: drivers of litter decomposition in drylands. Progress in Botany. Springer, pp. 273–302.

Benjamini, Y., Hochberg, Y., 1995. Controlling the false discovery rate: a practical and powerful approach to multiple testing. J. R. Stat. Soc. Ser. B Methodol. 57, 289–300.

Berenstecher, P., Vivanco, L., Pérez, L.I., Ballaré, C.L., Austin, A., 2020. Sunlight doubles aboveground carbon loss in a seasonally dry woodland in Patagonia. Curr. Biol. 30, 1–9.

Brandt, L., Bohnet, C., King, J., 2009. Photochemically induced carbon dioxide production as a mechanism for carbon loss from plant litter in arid ecosystems. J. Geophys. Res. Biogeosci. 114, G02004.

Čada, V., Morrissey, R.C., Michalová, Z., Bače, R., Janda, P., Svoboda, M., 2016. Frequent severe natural disturbances and non-equilibrium landscape dynamics shaped the mountain spruce forest in Central Europe. For. Ecol. Manag. 363, 169–178.

Day, T.A., Bliss, M.S., 2020. Solar photochemical emission of CO2 from leaf litter: sources and significance to C loss. Ecosystems 1–18.

Day, T.A., Bliss, M.S., 2019. A spectral weighting function for abiotic photodegradation based on photochemical emission of CO2 from leaf litter in sunlight. Biogeochemistry 146, 173–190.

Day, T.A., Guénon, R., Ruhland, C.T., 2015. Photodegradation of plant litter in the Sonoran Desert varies by litter type and age. Soil Biol. Biochem. 89, 109–122.
Durand, M., Murchie, E., Lindfors, A., Urban, O., Aphalo, P.J., Robson, T.M., 2021. Diffuse solar radiation and canopy photosynthesis in a changing environment. Agric. For. Meteorol. 311, 108684.
Flint, S.D., Caldwell, M.M., 1998. Solar UV-B and visible radiation in tropical forest gaps: measurements partitioning direct and diffuse radiation. Glob. Chang. Biol. 4, 863–870.
Foereid, B., Bellarby, J., Meier-Augenstein, W., Kemp, H., 2010. Does light exposure make plant litter more degradable? Plant Soil 333, 275–285.
Foereid, B., Rivero, M.J., Primo, O., Ortiz, I., 2011. Modelling photodegradation in the global carbon cycle. Soil Biol. Biochem. 43, 1383–1386.
Fukushima, R.S., Hatfield, R.D., 2001. Extraction and isolation of lignin for utilization as a standard to determine lignin concentration using the acetyl bromide spectrophotometric method. J. Agric. Food Chem. 49, 3133–3139.
Gallo, M.E., Porras-Alfaro, A., Odenbach, K.J., Sinsabaugh, R.L., 2009. Photoacceleration of plant litter decomposition in an arid environment. Soil Biol. Biochem. 41, 1433–1441.
Gallo, M.E., Sinsabaugh, R.L., Cabaniss, S.E., 2006. The role of ultraviolet radiation in litter decomposition in arid ecosystems. Appl. Soil Ecol. 34, 82–91.
Gliksman, D., Rey, A., Seligmann, R., Dumbur, R., Sperling, O., Navon, Y., Haenel, S., De Angelis, P., Arnone, J.A., Grunzweig, J.M., 2017. Biotic degradation at night, abiotic degradation at day: positive feedbacks on litter decomposition in drylands. Glob. Chang. Biol. 23, 1564–1574.
Hartikainen, S.M., Jach, A., Grané, A., Robson, T.M., 2018. Assessing scale-wise similarity of curves with a thick pen: as illustrated through comparisons of spectral irradiance. Ecol. Evol. 8, 10206–10218.
Hertel, C., Leuchner, M., Menzel, A., 2011. Vertical variability of spectral ratios in a mature mixed forest stand. Agric. For. Meteorol. 151, 1096–1105.
Hertel, C., Leuchner, M., Rotzer, T., Menzel, A., 2012. Assessing stand structure of beech and spruce from measured spectral radiation properties and modeled leaf biomass parameters. Agric. For. Meteorol. 165, 82–91.
Hothorn, T., Bretz, F., Westfall, P., 2008. Simultaneous inference in general parametric models. J. Math. Methods Biosci. 50, 346–363.
Iiyama, K., Wallis, A.F., 1990. Determination of lignin in herbaceous plants by an improved acetyl bromide procedure. J. Sci. Food Agric. 51, 145–161.
Keiser, A.D., Warren, R., Filley, T., Bradford, M.A., 2021. Signatures of an abiotic decomposition pathway in temperate forest leaf litter. Biogeochemistry 153, 177–190.
Keyser, P., Kirk, T., Zeikus, J., 1978. Ligninolytic enzyme system of phanaerochaete chrysosporium: synthesized in the absence of lignin in response to nitrogen starvation. J. Bacteriol. 135, 790–797.
King, J.Y., Brandt, L.A., Adair, E.C., 2012. Shedding light on plant litter decomposition: advances, implications and new directions in understanding the role of photodegradation. Biogeochemistry 111, 57–81.
Lin, Y., Karlen, S.D., Ralph, J., King, J.Y., 2018. Short-term facilitation of microbial litter decomposition by ultraviolet radiation. Sci. Total Environ. 615, 838–848.
Lin, Y., King, J.Y., 2014. Effects of UV exposure and litter position on decomposition in a California grassland. Ecosystems 17, 158–168.
Liu, G.F., Wang, L., Jiang, L., Pan, X., Huang, Z.Y., Dong, M., Cornelissen, J.H.C., 2018. Specific leaf area predicts dryland litter decomposition via two mechanisms. J. Ecol. 106, 218–229.
Ma, Z., Yang, W., Wu, F., Tan, B., 2017. Effects of light intensity on litter decomposition in a subtropical region. Ecosphere 8, e01770 01710.01002/ecs01772.01770.
Manzoni, S., Jackson, R.B., Trofymow, J.A., Porporato, A., 2008. The global stoichiometry of litter nitrogen mineralization. Science 321, 684–686.
Marinho, O.A., Martinelli, L.A., Duarte-Neto, P.J., Mazzi, E.A., King, J.Y., 2020. Photodegradation influences litter decomposition rate in a humid tropical ecosystem, Brazil. Sci. Total Environ. 715, 136601.
Mao, B., Zhao, L., Zhao, Q., Zeng, D., 2018. Effects of ultraviolet (UV) radiation and litter layer thickness on litter decomposition of two tree species in a semi-arid site of Northeast China. J. Arid Land 10, 416–428.
Masaki, T., Matsuura, Y., Takahashi, M., 2002. Effect of Soil Conditions on the Distribution and Growth of Trees, Diversity and Interaction in a Temperate Forest Community. Springer, pp. 81–91.
Méndez, M.S., Martinez, M.L., Araujo, P.I., Austin, A.T., 2019. Solar radiation exposure accelerates decomposition and biotic activity in surface litter but not soil in a semiarid woodland ecosystem in Patagonia, Argentina. Plant Soil 445, 483–496.
Nakashizuka, T., Matsumoto, Y., 2002. Diversity and Interaction in a Temperate Forest Community: Ogawa Forest Reserve of Japan. Springer Science & Business Media.
Navrátil, M., Špunda, V., Marková, I., Janouš, D., 2007. Spectral composition of photosynthetically active radiation penetrating into a Norway spruce canopy: the opposite dynamics of the blue/red spectral ratio during clear and overcast days. Trees 21, 311–320.
Neale, R., Barnes, P., Robson, T., Neale, P., Williamson, C., Zepp, R., et al., 2021. Environmental effects of stratospheric ozone depletion, UV radiation, and interactions with climate change: UNEP environmental effects assessment panel, update 2020. Photochem. Photobiol. Sci. 20, 1–67.
Osono, T., Takeda, H., 2001. Organic chemical and nutrient dynamics in decomposing beech leaf litter in relation to fungal ingrowth and succession during 3-year decomposition processes in a cool temperate deciduous forest in Japan. Ecol. Res. 16, 649–670.
Pancotto, V.A., Sala, O.E., Cabello, M., Lopez, N.I., Matthew Robson, T., Ballaré, C.L., Caldwell, M.M., Scopel, A.L., 2003. Solar UV-B decreases decomposition in herbaceous plant litter in Tierra del Fuego, Argentina: potential role of an altered decomposer community. Glob. Chang. Biol. 9, 1465–1474.
Parton, W., Silver, W.L., Burke, I.C., Grassens, L., Harmon, M.E., Currie, W.S., King, J.Y., Adair, E.C., Brandt, L.A., Hart, S.C., 2007. Global-scale similarities in nitrogen release patterns during long-term decomposition. Science 315, 361–364.
Pei, G., Liu, J., Peng, B., Gao, D., Wang, C., Dai, W., Jiang, P., Bai, E., 2019. Nitrogen, lignin, C/N as important regulators of gross nitrogen release and immobilization during litter decomposition in a temperate forest ecosystem. For. Ecol. Manag. 440, 61–69.
Pieristè, M., Chauvat, M., Kotilainen, T.K., Jones, A.G., Aubert, M., Robson, M.T., Forey, E., 2019. Solar UV-A radiation and blue light enhance tree leaf litter decomposition in a temperate forest. Oecologia 191, 191–203.
Pieristè, M., Forey, E., Sahraoui, A.L.-H., Meglouli, H., Laruelle, F., Delporte, P., Robson, T.M., Chauvat, M., 2020a. Spectral composition of sunlight affects the microbial functional structure of beech leaf litter during the initial phase of decomposition. Plant Soil 515–530.
Pieristè, M., Neimane, S., Solanki, T., Nybakken, L., Jones, A.G., Forey, E., Chauvat, M., Ņečajeva, J., Robson, T.M., 2020b. Ultraviolet radiation accelerates photodegradation under controlled conditions but slows the decomposition of senescent leaves from forest stands in southern Finland. Plant Physiol. Biochem. 146, 42–54.
Predick, K.I., Archer, S.R., Aguillon, S.M., Keller, D.A., Throop, H.L., Barnes, P.W., 2018. UV-B radiation and shrub canopy effects on surface litter decomposition in a shrub-invaded dry grassland. J. Arid Environ. 157, 13–21.
Schlesinger, W.H., Bernhardt, E.S., 2013. Biogeochemistry: An Analysis of Global Change. Academic press.
Song, X., Peng, C., Jiang, H., Zhu, Q., Wang, W., 2013. Direct and indirect effects of UV-B exposure on litter decomposition: a meta-analysis. PLoS One 8, e68858–e68859.
Song, X.Z., Jiang, H., Zhang, H.L., Peng, C.H., Yu, S.Q., 2011. Elevated UV-B radiation did not affect decomposition rates of needles of two coniferous species in subtropical China. Eur. J. Soil Biol. 47, 343–348.
Song, X.Z., Zhang, H.L., Jiang, H., Peng, C.H., 2014. Combination of nitrogen deposition and ultraviolet-B radiation decreased litter decomposition in subtropical China. Plant Soil 380, 349–359.
Sulzberger, B., Austin, A.T., Cory, R.M., Zepp, R.G., Paul, N.D., 2019. Solar UV radiation in a changing world: roles of cryosphere–land–water–atmosphere interfaces in global biogeochemical cycles. Photochem. Photobiol. Sci. 18, 747–774.
Sun, T., Dong, L.L., Wang, Z.W., Lü, X.T., Mao, Z.J., 2016. Effects of long-term nitrogen deposition on fine root decomposition and its extracellular enzyme activities in temperate forests. Soil Biol. Biochem. 93, 50–59.
Swift, M.J., Heal, O.W., Anderson, J., 1979. Decomposition in Terrestrial Ecosystems. Univ of California Press.
Uselman, S.M., Snyder, K.A., Blank, R.R., Jones, T.J., 2011. UVB exposure does not accelerate rates of litter decomposition in a semi-arid riparian ecosystem. Soil Biol. Biochem. 43, 1254–1265.
Verhoef, H.A., Verspagen, J.M.H., Zoomer, H.R., 2000. Direct and indirect effects of ultraviolet-B radiation on soil biota, decomposition and nutrient fluxes in dune grassland soil systems. Biol. Fertil. Soils 31, 366–371.
Wallace, K., Laughlin, D.C., Clarkson, B.D., Schipper, L.A., 2018. Forest canopy restoration has indirect effects on litter decomposition and no effect on denitrification. Ecosphere 9, e02534.
Wang, J., Liu, L., Wang, X., Chen, Y., 2015. The interaction between abiotic photodegradation and microbial decomposition under ultraviolet radiation. Glob. Chang. Biol. 21, 2095–2104.
Wang, Q.-W., Pieristè, M., Liu, C., Kenta, T., Robson, M.T., Kurokawa, H., 2021. The contribution of photodegradation to litter decomposition in a temperate forest gap and understorey. New Phytol. 229, 2625–2636.
Wang, Q.-W., Robson, T.M., Pieristè, M., Oguro, M., Oguchi, R., Murai, Y., Kurokawa, H., 2020. Testing trait plasticity over the range of spectral composition of sunlight in forb species differing in shade tolerance. J. Ecol. 108, 1923–1940.
Yeo, I.K., Johnson, R.A., 2000. A new family of power transformations to improve normality or symmetry. Biometrika 87, 954–959.